



Scholars Research Library

Der Pharma Chemica, 2015, 7(9):161-164  
(<http://derpharmachemica.com/archive.html>)



ISSN 0975-413X  
CODEN (USA): PCHHAX

## Preparation and characterization of anodic oxide film on aluminum by pulse current anodizing

Hadi Adelkhani\* and Hamzeh Forati Rad

Nuclear Fuel Cycle School, NSTRI, Tehran, Iran

### ABSTRACT

The present study examined the influence of pulse current parameters on the characteristics of anodized aluminum anodic film. The baths contained  $H_2SO_4$  (10% ww) and bath volume was 1 L. Anodizing was carried out for 30 min at a current density of  $1.0 A/dm^2$  and bath temperature of  $10^\circ C$ . The anodic film was affected by electrolyte power dissolution and the length of time the anodic film was in contact with the electrolyte without applied current. The results confirmed that the cell nano-structure of anodic film is approximately hexagonal. The structure was strongly affected by the frequency and duty cycle of the pulse current.

**Keywords:** Anodizing, Aluminum, Pulse current, Anodic film

### INTRODUCTION

Aluminium is remarkable for the metal's low density and for its ability to resist corrosion due to the phenomenon of passivation. Anodizing is an effective method for passivation of Al and enhancing protection against corrosion and the decorative behavior of aluminum and other metals. The anodic reaction is the oxidation of aluminum ( $Al \rightarrow Al^{3+} + 3e^-$ ). In this method, aluminum was used as an anode in  $H_2SO_4$ ,  $H_2C_2O_4$ , and  $H_3PO_4$  electrolytes. In the initial stages, the aluminum cation ( $Al^{3+}$ ) reacted with an oxygen anion ( $O_2^-$ ) to form  $Al_2O_3$  as the oxide film ( $2Al^{3+} + 3O_2^- \rightarrow Al_2O_3$ ). As anodizing continued, the growing  $Al_2O_3$  film competed with the dissolution reaction of the electrolytes ( $Al_2O_3 + 6H^+ \rightarrow 2Al^{3+}_{(aq)} + 3H_2O$ ). Electrolytes attacked the barrier layer at separate points, producing a porous film structure. The idealized anodic film had a uniform hexagonal cellular (anodic cells) structure with a central pore in each cell (Figure 1), but most anodizing conditions produced film with less uniformity. It is well known that anodizing conditions (current, voltage, temperature, electrolyte composition) affect anodic cell structural parameters and properties [1-7].

Direct current (DC) is normally used in anodizing and other electrochemical processes, such as electroplating, electroforming, electro-polishing, electro-machining and electrochemical synthesis. A more recent option is the use of a pulse current (PC) in the electrochemical process [8-12]. The main parameters of PC are on-time ( $t_{on}$ ), off-time

( $t_{off}$ ), frequency ( $f$ ), and duty cycle ( $\theta$ ). The relations between these parameters are defined as  $f = \frac{1}{t_{on} + t_{off}}$  and

$\theta = \frac{t_{on}}{t_{on} + t_{off}} \times 100$ . The pulse current strongly influences the characteristics of the final product of the electrochemical process. A number of studies have used PC for anodizing [3, 12-15].

In the present study, the permanent anodizing conditions of voltage, temperature, electrolyte composition, and the effects of pulse parameters on the uniformity, dimension, and distribution of anodic cells was investigated.

## MATERIALS AND METHODS

The anode was prepared using AA1070 aluminum alloy sheets with dimensions of  $13 \times 5 \text{ cm}^2$ . The samples were first degreased with acetone and then with NaOH solution. The samples were chemically polished in  $\text{NaNO}_3\text{-H}_3\text{PO}_4\text{-HNO}_3$  solution and were desmutted using  $\text{HNO}_3$  solution. The samples were finally rinsed using double-distilled water.

The anodizing electrolyte was  $\text{H}_2\text{SO}_4$  (10% ww). Anodizing was carried out for 30 min at a current density of  $1.0 \text{ A/dm}^2$  and a bath temperature of  $10^\circ\text{C}$ . X-ray diffraction (XRD: Philips with Cu K $\alpha$  radiation, 30 kV) was used to analyze the structure and the phases present in the anodic film. Scanning electron microscopy (SEM) and energy dispersive x-ray analysis (EDX: Philips XI30) were used to study the microstructure and morphology of the anodic films. For details of the experimental conditions, refer to reference 3.

## RESULTS AND DISCUSSION

The SEM images of samples prepared under different conditions are shown in Figure 2. Although anodic cells were present on the surface of all samples, the uniformity of the anodic cells strongly depended on the frequency, duty cycle, and type of current (PC or DC).

### 3.1. $f = 100 \text{ Hz}$ and $\theta = 40\%$ , $50\%$ and $70\%$

The uniformity of the anodic cells decreased as the duty cycles increased from 40% to 70%. The shapes and borders of the anodic cells are very clear at low duty cycles, but faded as the duty cycle increased. These differences are related to the off-time and the probability of anodic film dissolving during the off-time. The off-time at  $f = 100 \text{ Hz}$  and  $\theta = 40\%$  is 6 ms, at  $f = 100 \text{ Hz}$  and  $\theta = 50\%$  is 5 ms, and at  $f = 100 \text{ Hz}$  and  $\theta = 70\%$  is 3 ms. Increasing the duty cycle from 50% to 70% decreased the off-time, decreasing the probability of anodic film dissolving.

At  $f = 100 \text{ Hz}$  and  $\theta = 40\%$ , the probability of anodic film dissolution is high for a long off-time. The SEM image shows many pores in the anodic film. No pores can be seen in the anodic film samples at  $f = 100 \text{ Hz}$  and  $\theta = 50\%$  or  $f = 100 \text{ Hz}$  and  $\theta = 70\%$ . The SEM image of  $f = 100 \text{ Hz}$  and  $\theta = 70\%$  shows that the dissolution rate of the barrier layer was low and the shapes and borders of the anodic cells are not clear.

The thickness of the anodic film increased as the duty cycle increased. The thickness of the samples at  $f = 100 \text{ Hz}$  and  $\theta = 40\%$  was  $4 \mu\text{m}$ , at  $f = 100 \text{ Hz}$  and  $\theta = 50\%$  was  $8 \mu\text{m}$ , and  $f = 100 \text{ Hz}$  -  $\theta = 70\%$  was  $15 \mu\text{m}$ . For a short off-time, the rate of dissolution of the anodic film decreased, so the thickness increased. Consequently, anodic film prepared at  $f = 100 \text{ Hz}$  and  $\theta = 70\%$  is thicker than other samples prepared by PC anodizing. The thickness of the PC sample at  $f = 100 \text{ Hz}$  and  $\theta = 70\%$  was lower than that of the DC sample.

### 3.2. $\theta = 50\%$ and $f = 100, 500, \text{ and } 1000 \text{ Hz}$

The SEM images of samples prepared at the same duty cycle ( $\theta = 50\%$ ) and different frequencies ( $f = 100, 500$  and  $1000 \text{ Hz}$ ) are shown in Figures 2(a), 2(d), and 2(e). As seen, the uniformity of the anodic cell increased as the frequency increased from 100 Hz to 1000 Hz. The sample at  $f = 1000 \text{ Hz}$  and  $\theta = 50\%$  shows anodic cells with very sharp borders. By contrast, the thickness of the anodic film decreased as frequency increased. The thickness of the anodic film at  $f = 500 \text{ Hz}$  and  $\theta = 50\%$  was  $5 \mu\text{m}$  and at  $f = 1000 \text{ Hz}$  and  $\theta = 50\%$  was  $4 \mu\text{m}$ .

### 3.3. DC

The SEM image of the sample prepared using DC current is shown in Figure 2(f). The thickness of the sample is higher than for the PC samples at  $25 \mu\text{m}$ . The SEM image confirms that the borders of the anodic cells are not very

clear. The absence of off-time in DC anodizing is a major reason for the increased thickness and effected the morphology of the anodic film.

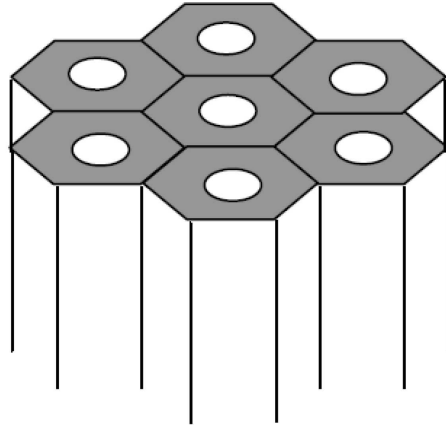


Figure 1 - idealized structure of anodic cells obtain by anodizing of aluminum

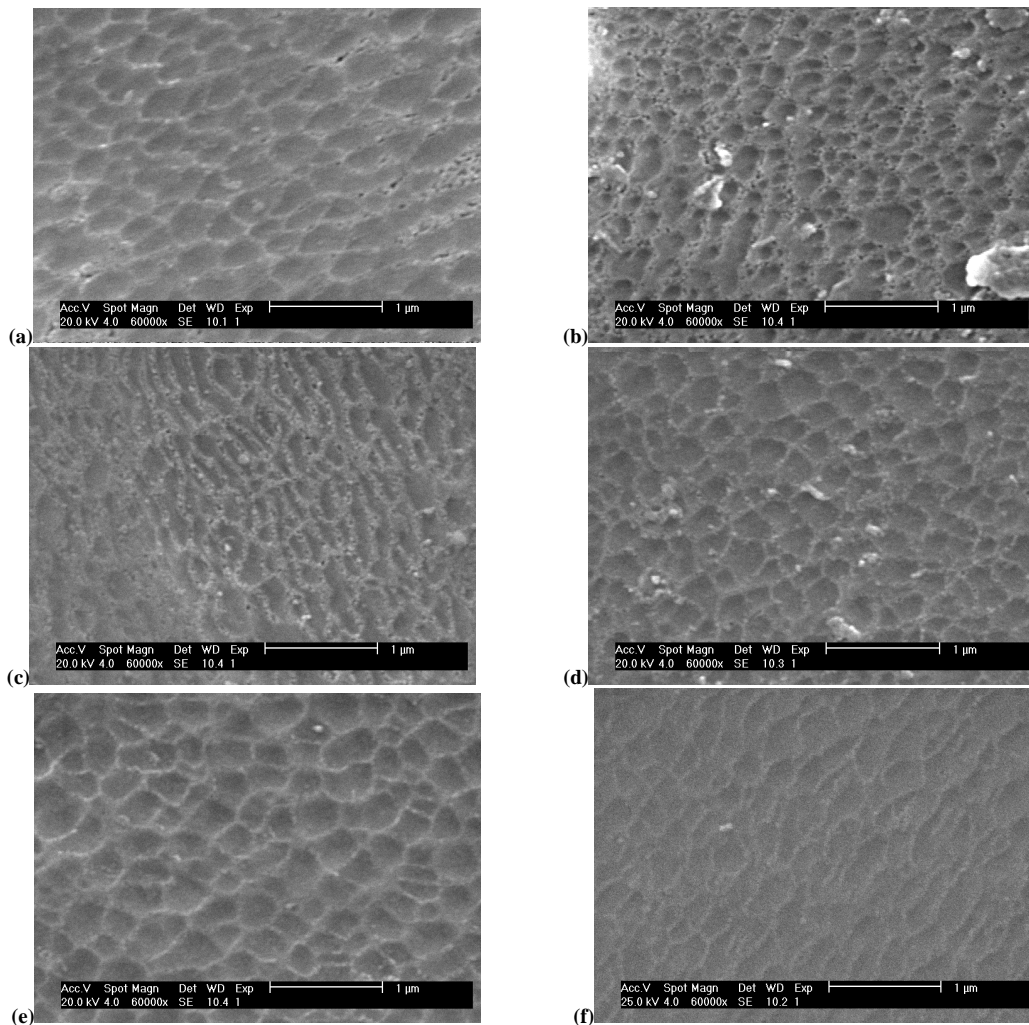


Figure 2 -The SEM images of samples prepare at variant conditions: (a)  $f=100 \text{ Hz}-\theta=40\%$ , (b)  $f=100 \text{ Hz}-\theta=50\%$ , (c)  $f=100 \text{ Hz}-\theta=70\%$ , (d)  $f=500 \text{ Hz}-\theta=50\%$ , (e)  $f=1000 \text{ Hz}-\theta=50\%$ , and (f) DC

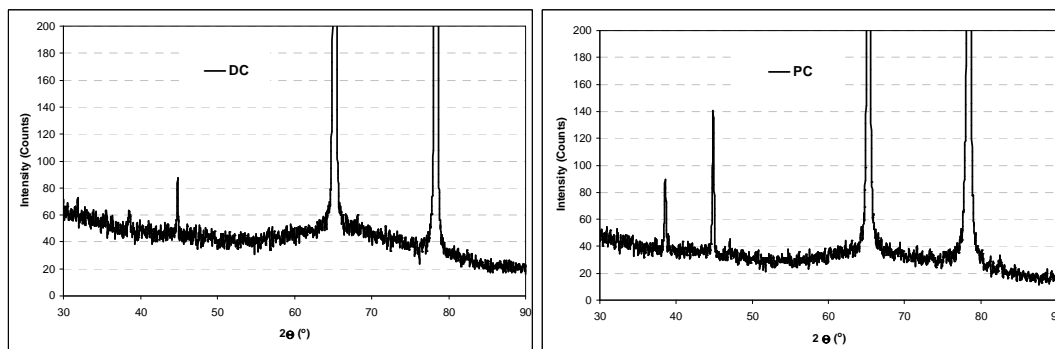


Figure 3- XRD pattern of anodic film formed on AA1070 Al alloy under different anodizing process: (DC) direct current; (PC) pulse current  $f=500$  Hz,  $\theta=70\%$

### 3.4. Crystal structure

XRD was used to determine the crystal structure of the anodic film. The results of this analysis for the DC and PC samples at  $f = 500$  Hz and  $\theta = 70\%$  are shown in Figure 3. The  $\alpha$ - $\text{Al}_2\text{O}_3$  shows a peak at  $38^\circ$  and  $\gamma$ - $\text{Al}_2\text{O}_3$  shows a peak at  $44.8^\circ$ . XRD confirmed that there is only one peak at  $\gamma$ - $\text{Al}_2\text{O}_3$  for the DC sample, but there are two peaks at  $\gamma$ - $\text{Al}_2\text{O}_3$  and  $\alpha$ - $\text{Al}_2\text{O}_3$  for the PC sample.

The occurrence of different crystalline aluminum oxide phases in anodic film from anodizing has been previously reported [1, 16]. The intensity of the peaks for the PC sample was greater than for the DC sample. This suggests that a fine-grained crystalline phase has formed during PC anodizing. Because the anodic film is not as thick as the AA1070 Al substrate, the diffraction peaks of the Al alloy substrate are reflected in the XRD pattern ( $2\theta = 67^\circ$  and  $2\theta = 78^\circ$ ).

## CONCLUSION

The SEM images confirm that all samples are approximately hexagonal in structure. This structure and its uniformity are strongly affected by the frequency and duty cycle of the PC. In anodizing, two processes are essential and competitive: the growth and dissolution of  $\text{Al}_2\text{O}_3$  film. The off-time ( $T_{\text{off}}$ ) balances these processes and the thickness of the anodic film depends on off-time.

## REFERENCES

- [1] Parekh S P, Pandya A V, Kadiya H K, *Der Pharma Chemica*, **2013**, 5, 125
- [2] Christoulaki A, Dellis S, Spiliopoulos N, Anastassopoulos D L, Vradis A A, *J. Appl. Electrochem.*, **2014**, 44, 701.
- [3] Adelkhani H, Forati Rad H, *Iranian Journal of Surface and Engineering*, **2013**, 16, 9.
- [4] Luo S L, Tang H, Zhou H H, Chen J H, Kuang Y F, *Surf. Coat. Tech.*, **2003**, 168, 91.
- [5] Araoyinbo A O, Ahmad Fauzi M N, Sreekantan S, Aziz A, *J. Non-Cryst. Solids*, **2010**, 356, 1057.
- [6] Vrublevsky I A, Chernyakova K V, Ispas A, Bund A, Zavadski S, *Thin Solid Films*, **2014**, 556, 230.
- [7] Ghorbani M, Nasirpouri F, Iraj Zad A, Saedi A, *Mater. Design*, **2006**, 27, 983.
- [8] Alfantazi A M, Erb U, *Corrosion*, **1996**, 52, 880.
- [9] Adelkhani H, Arshadi M R, *J. Alloy. Compd.*, **2009**, 476, 234.
- [10] Bhuyan A, Gregory B, Lei H, Seow Y Y, *Sensors*, **2005** IEEE, Conference 314 – 317, Irvine, CA.
- [11] Chung C K, Chang W T, Liao M W, Chang H C, *Mater. Lett.*, **2012**, 88, 104.
- [12] Adelkhani H, Ghaemi M, *Solid State Ionics*, **2008**, 179, 2278.
- [13] Rasmussen J J, U.S. Patent, **2000**, 6113770
- [14] Fratila-Apachitei L E, Duszczyc J, Katgerman L, *Surf. Coat. Tech.*, **2003**, 165 232.
- [15] Chung C K, Liao M W, Chang H C, Chang W T, Liu T Y, *Microsyst. Technol.*, **2013**, 19, 387.
- [16] Lomov A A, Karavanskiĭ V A, Vasil'ev A L, Novikov D V, *Crystallogr. Reports*, **2008**, 53, 742.